JOURNAL OF PROPULSION AND POWER
Vol. 22, No. 3, May–June 2006

Technical Notes

TECHNICAL NOTES are short manuscripts describing new developments or important results of a preliminary nature. These Notes should not exceed 2500 words (where a figure or table counts as 200 words). Following informal review by the Editors, they may be published within a few months of the date of receipt. Style requirements are the same as for regular contributions (see inside back cover).

Effect of Hall Currents on Simulated Three-Dimensional Scramjet with Magnetohydrodynamic Bypass

Datta V. Gaitonde*
Air Force Research Laboratory,
Wright–Patterson AFB, Ohio 45433

I. Introduction

In an earlier effort,[1,2] a verified high-resolution numerical approach was employed to explore the kinematic and dynamic structure of the flowfield in a generic, dual-plane mixed compression scramjet configuration at Mach 8, with and without magnetohydrodynamic (MHD) bypass. A generator and an accelerator were mounted in converging and diverging ducts, respectively, straddling a constant cross-sectional area combustion chamber, as shown in Fig. 1. Both components were assumed to operate in Faraday mode, with coarsely segmented side-wall mounted electrodes.

The simulated flow was seen to be dominated by various complicated three-dimensional features, including particularly swept shock-wave/boundary-layer interactions separation and vortical structures, whose impact on the current, electric, and ponderomotive force fields was significant and confirmed the inadequacy of two-dimensional and inviscid analyses. Overall, the magnetohydrodynamics (MGD) generator exhibited the potential to efficiently slow down flow in the inlet, thus decreasing scramjet inlet length, and to reduce the total temperature of the flow. However, three-dimensional separation engendered limitations on the useful length of the generator by inducing near-wall secondary eddy currents and local body force reversal. On the other hand, accelerator operation was characterized by more prominent irreversibilities, especially near walls, where large electric and ponderomotive force field gradients were observed. Other aspects, including those related to integrated parameters such as lift and thrust, may be found in Refs. 1 and 2.

The high-altitude operating environment of scramjet inlets has been characterized in several works.[3,4] Essentially, the pressure is anticipated to be relatively low. Because the natural conductivity of air is small, artificial ionization enhancement incurs an energy penalty and levels will be low. Even with relatively efficient nonequilibrium techniques, such as e-beams or pulsed electric fields, the electrical conductivity, σ, is anticipated to be small, of order 1 mho/m. To compensate, the imposed magnetic field must be large enough to result in an interaction parameter of order unity. Under these conditions, the Hall effect, primarily that associated with electrons, is important. A recent detailed experimental and theoretical study[5] confirms previous assessments on the importance of Hall currents. The effect, proportional to the ratio of the cyclotron (or Larmor) and collision frequencies, is measured in terms of a reference Hall parameter, $R_H = \sigma_{\text{ref}}\beta_{\text{ref}}B_{\text{ref}}$, where β is the Hall coefficient, B is the magnetic induction, and subscript ref denotes reference values. Although the segmented electrode configuration shown in Fig. 1 inhibits the deleterious effects of Hall currents on MGD devices operating in the Faraday configuration, complete annihilation does not occur, particularly with coarse segmentation such as that explored here (Fig. 1). The purpose of this note is to extend the results of Refs. 1 and 2 to include an analysis of impact of Hall currents on MHD component operation. Given the phenomenological elements of the theoretical model employed, it is emphasized that the principal objective is to characterize the anticipated trends in a qualitative rather than a quantitative sense.

II. Governing Equations and Numerical Procedure

Details of the governing equations are provided in Ref. 1, and are only summarized here. Basically, the full three-dimensional Navier–Stokes equations are solved, together with a source-term formulation of the electromagnetic terms. The Roe flux-difference split method is employed for inviscid components, whereas viscous terms are centered. An implicit approximately factored approach is utilized for efficient time integration.

The principal electromagnetic quantities are the magnetic field, the electric current vector, and the electric field. The magnetic field is assumed to be uniform, pointing in the y direction (see Fig. 1), and unperturbed by the interaction. This implies that the magnetic Reynolds number is small—an assumption whose validity is justified in system-level and parametric studies.[3]

The effects associated with Hall currents are incorporated through the expression for electric current, $\boldsymbol{j}$, estimated from the generalized Ohm's law[6]:

$$\boldsymbol{j} = \sigma[\boldsymbol{E} + \boldsymbol{U} \times \boldsymbol{B} - \beta(\boldsymbol{j} \times \boldsymbol{B}) + \alpha(\boldsymbol{j} \times \boldsymbol{B} \times \boldsymbol{B})] \qquad (1)$$

where β and α are the (electron) Hall and ion-slip coefficients, respectively, and $\boldsymbol{E}$ is the electric field vector. Although only the electron Hall effect is considered in this paper, the ion-slip term, whose impact is expected to be less dominant, is carried through for future reference. Based on the arguments listed in Ref. 6, the

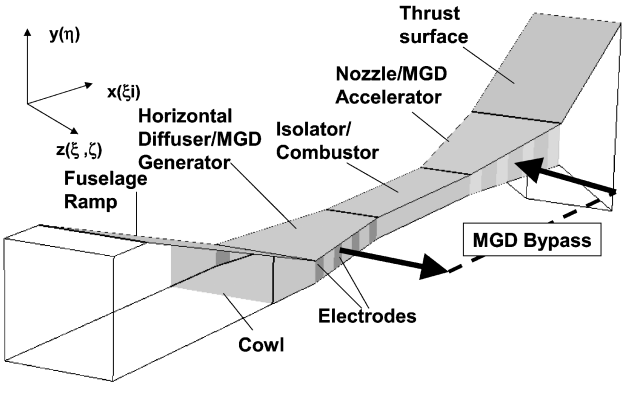

Fig. 1 Dual-plane compression flow-through scramjet configuration. Aspect ratio is 1:2:2.

Received 17 November 2004; revision received 26 September 2005; accepted for publication 26 September 2005.

*Technical Area Leader, Computational Sciences Branch, Aeronautical Sciences Division, Air Vehicles Directorate. Associate Fellow AIAA.

reasonable assumption is made that terms due to electron pressure gradient are negligible. Equation (1) is an implicit relation that may be solved for $\boldsymbol{j}$ in terms of a tensor conductivity, $\bar{\bar{\sigma}}$:

$$\boldsymbol{j} = \bar{\bar{\sigma}}[\boldsymbol{E} + \boldsymbol{U} \times \boldsymbol{B}] \tag{2}$$

Detailed expressions for the components of $\bar{\bar{\sigma}}$ have been provided in Ref. (7). From a practical standpoint, it is more convenient to combine $\boldsymbol{j}$ with $\boldsymbol{B}$ and $\boldsymbol{E}$, respectively, to yield the body force, $\boldsymbol{j} \times \boldsymbol{B}$ appearing in the momentum equation and $\boldsymbol{E} \cdot \boldsymbol{j}$ in the energy equation:

$$\boldsymbol{j} \times \boldsymbol{B} = (Q/D)[(j \times B)_0 + I_s \alpha (j \times B)_\alpha + R_H \beta (j \times B)_\beta] \tag{3}$$

where $Q = \sigma_{\text{ref}} B_{\text{ref}}^2 L_{\text{ref}}/(\rho_{\text{ref}} U_{\text{ref}})$ is the interaction parameter, and $(j \times B)_0$, $(j \times B)_\alpha$, and $(j^* \times B^*)_\beta$ have been presented in Ref. 7. For example,

$$(j \times B)_\alpha = \sigma^2 \boldsymbol{B}^2 [\boldsymbol{E} \times \boldsymbol{B} - \boldsymbol{B}^2 \boldsymbol{U} + (\boldsymbol{B} \cdot \boldsymbol{U})\boldsymbol{B}] \tag{4}$$

Complete expressions for $(E \cdot j)$ may also be found in Ref. 7. Finally, the electric field is obtained by solving the current continuity equation, $\nabla \cdot \boldsymbol{j} = 0$. Upon introduction of a scalar electric potential, a Poisson equation is obtained, which is solved with an approximately factored method as described in Ref. 8.

Spatially variable combustion and plasma parameters are either specified or phenomenologically derived in the manner of Ref. 1. In particular, electrical conductivity is assumed to exhibit spatial variation compatible with an e-beam nonequilibrium ionization method. Fluid dynamic variables are specified in the standard manner, including no-slip and zero normal pressure gradient, and the walls are assumed to be adiabatic. At electrode boundaries, the potential is enforced so that the load factor is 0.8 in the generator and 1.2 in the accelerator, based on average values of velocity in each component and on the distance between electrodes.[1] At insulators, the normal component of electric current is set to zero. The Hall effect in particular yields significant electric field build-up at the edges of electrodes, requiring special numerical procedures, as described in Ref. 8.

III. Results

The freestream flow parameters were assumed to be Mach number, $M = 8$ and Reynolds number, $Re = 1.6 \times 10^6$ based on the upstream width of the configuration, which is set at 0.6 m. The interaction parameter, Q, and the Hall parameter, R_H, were set to unity, consistent with order of magnitude values selected in system studies. As noted earlier, all other quantities are maintained to be the same as in Refs. 1, 2 to facilitate direct comparison.

The effect of Hall currents may be characterized in terms of local and global aspects. Broadly speaking, there are two major effects of the Hall current. First, although the configuration is symmetric about the vertical plane, the Hall effect gives rise to significant flow asymmetry about that plane. Second, and partly as a consequence of the first effect, the evolution of the vortical structures observed as a result of flow separation is modified in a striking fashion.

The development of asymmetry is shown in Fig. 2, which depicts Mach contours at several crossflow planes along the axis of the scramjet without (Fig. 2a) and with (Fig. 2b) Hall terms. The vortical structure in both cases is initiated in the same manner, through separation of the upper and lower wall boundary layers because of swept shock/boundary layer interactions in the converging section of the inlet. Whereas in the absence of Hall effects the upper and lower vortical structures are symmetric about the vertical center plane, a distinctly skewed pattern results when Hall currents are included in the analysis. Here, the upper and lower structures do not grow to encompass the height of the channel. Rather, they are compressed and are seen to move to the left of the centerline. New shock structures whose genesis is explained further below evoke a sidewall shock/boundary layer interaction that is absent when Hall effects are neglected. These in turn induce boundary layer separation on the sidewall, in addition to that on the lower and upper walls. The result of this is most evident at the end of the combustor, where

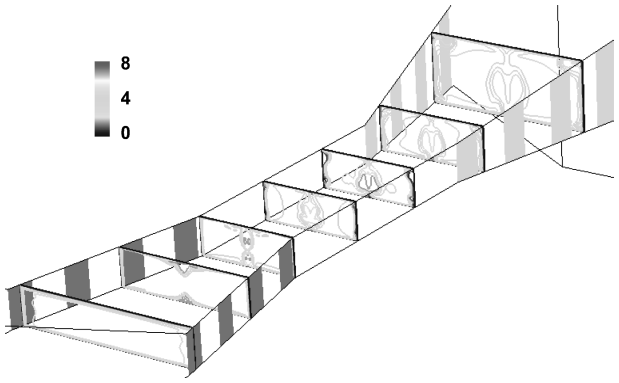

a) No Hall effect

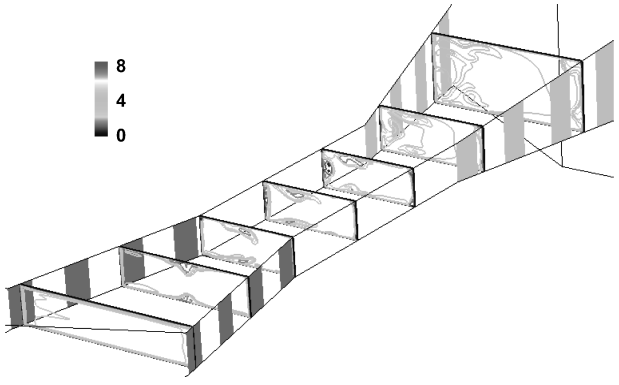

b) With Hall effect

Fig. 2 Mach contours on several cross-sectional planes.

three structures are visible, one on each of the upper, lower, and left sidewalls.

The development of a streamwise component to the electric field—the Hall field—has a profound impact on the current pattern, and consequently on the body force and thus fluid on dynamic variables such as pressure and velocity. To illustrate, the current pattern in the generator segment, computed with the tensor conductivity, is shown in Fig. 3. In the vicinity of the first electrode, the current flows in the direction of $\boldsymbol{U} \times \boldsymbol{B}$ because the load factor is less than unity. However, a streamwise component is clearly evident at subsequent electrodes. For example, the current line emerging from the downstream edge of the second cathode (the left electrode looking downstream) enters the third anode. This effect disappears for the fourth pair, where current is again transverse to the flow, because of the current continuity constraint. In the absence of Hall effects, it was shown in Ref. 1 that eddy currents are formed in the upper and lower vortical regions of Fig. 2a. These patterns are also influenced by the Hall field, as observed in Fig. 3a. Essentially, the recirculating patterns are stretched longitudinally to form spirals that do not close on themselves, but rather terminate at electrodes. Although not shown, current reversal near the upper and lower surfaces is maintained with Hall effects, but is even more confined near the surface because of the shallower nature of the vortical structures. Currents in the accelerator (not shown, for brevity; see Ref. 1) are affected in an analogous fashion. Because the nominal direction here is opposed to the $\boldsymbol{U} \times \boldsymbol{B}$ direction, the Hall field induces an upstream rather than downstream inclination, particularly near the entrance to the accelerator, where the MHD effect is high.[1]

The ponderomotive force pattern corresponding to the current field is shown in Fig. 3b, where again the situation in the generator is highlighted. Because a uniform vertically directed magnetic field has been assumed, the body force pattern can be determined by considering the current orientation. The axial component of current, pointing downstream, yields a spanwise component of force by virtue of its cross-product relationship to $\boldsymbol{j}$ and $\boldsymbol{B}$. This effect increases on proceeding downstream in the generator, and

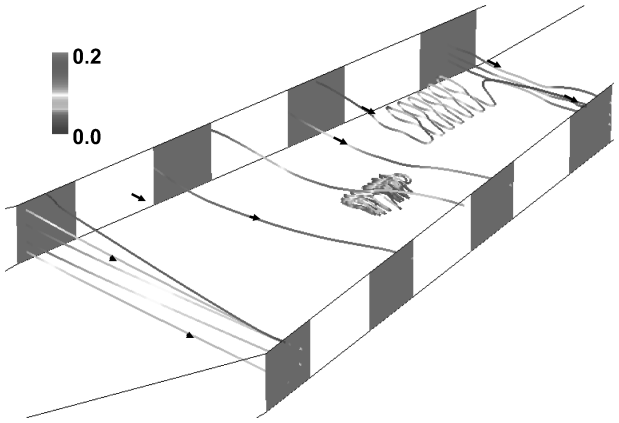

a) Current

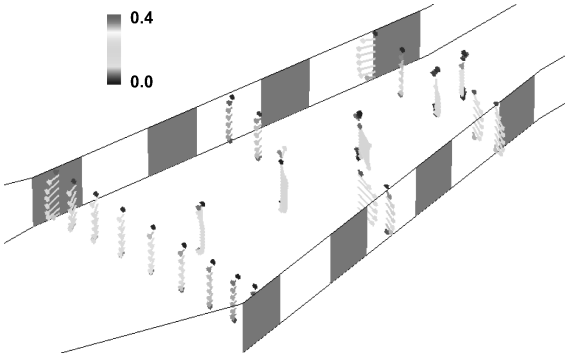

b) Ponderomotive force

Fig. 3 Impact of Hall effect on generator operation.

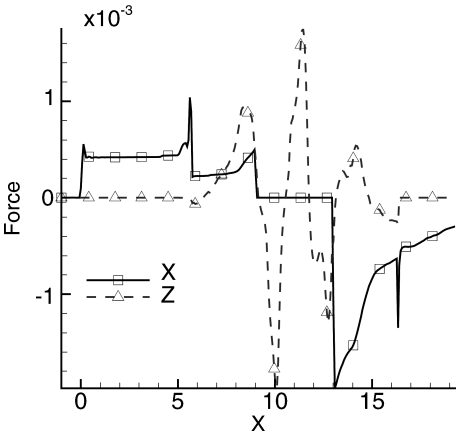

a) Pressure forces

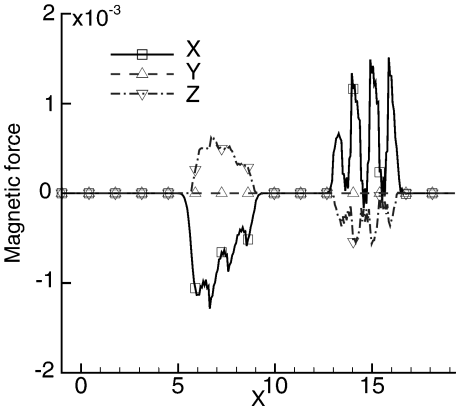

b) Magnetic forces

Fig. 4 Integrated forces with Hall effect.

is particularly pronounced in the midsection. The sideward force induces a component in the fluid motion toward the right wall, resulting in a system of waves. These waves reflect off the right wall and subsequently impact the left wall in the downstream combustor section. It is thus the evolution of this system with axial distance that ultimately yields the complex sequence of events associated with the sidewall shock/boundary layer interaction, including separation and the emergence of the asymmetric contour pattern observed in Fig. 2b.

The effect of flow asymmetry induced by the Hall effect on integrated pressure and magnetic forces is shown in Fig. 4. In this figure, the appropriate force is integrated over the cross-sectional area at each streamwise location. The streamwise pressure force variation (X), Fig. 4a, arises primarily from the top and bottom faces and is only slightly influenced by Hall terms. A similar observation may be made regarding Y forces, which are not shown. However, the significant effects are evident in the yaw force component (Z). The symmetry of the configuration about the vertical plane ensures that yaw forces are zero when Hall effects are ignored. However, asymmetry due to Hall effects impacts in all regions downstream of the generator, as the system of waves associated with the sideward evolves downstream. In the generator, the pressure force points in the positive Z direction as fluid is pushed against the right sidewall by the body force. Counter shock waves generated to align the velocity vector in the streamwise direction reflect back and forth between the left and right sidewalls, resulting in an oscillatory pattern as shown.

Magnetic forces computed by integrating $\boldsymbol{j} \times \boldsymbol{B}$ at each cross-sectional section and shown in Fig. 4b are also consistent with these observations. The streamwise force shows only modest change from that exhibited in Ref. 1, and the vertical force remains negligible even with the Hall effect, suggesting that the contribution of the Hall effect due to the main streamwise high-speed fluid motion is primary, whereas that associated with separation is secondary. In contrast, the spanwise force is now relatively large, pointing in the $+Z$ direction in the generator and $-Z$ direction in the accelerator. The Hall effect thus clearly demonstrates the potential to generate significant yawing integrated force and concommitant moment components, which must be factored into practical devices.

IV. Summary

Previously reported studies of a representative fully three-dimensional simulated scramjet configuration operating with MHD generator and accelerator components are extended to explore the effect of Hall currents. Segmented electrode Faraday operation is assumed. The main trends include the development of streamwise components of electric field, corresponding axial currents, and spanwise body force components. The effect of the body force is to generate a shock pattern originating in the generator and inducing separation of the sidewall layer on only the left side (looking downstream). The breakdown of vertical symmetry yields significant yawing components in both integrated pressure and magnetic forces. These results are intended to provide a qualitative assessment of Hall effects in a relatively long scramjet configuration and must be further analyzed to explore the effect of finer segmentation.

Acknowledgments

The author is grateful for Air Force Office of Scientific Research (AFOSR) sponsorship under tasks monitored by J. Schmisseur and F. Fahroo. This work was also supported in part by a grant of High Performance Computing (HPC) time from the U.S. Department of Defense (DoD) HPC Shared Resource Centers at Aeronautical Systems Center (ASC), Corps of Engineers, Waterways Experiment Station (CEWES) and Naval Oceanographic Office (NAVO).

References

[1]Gaitonde, D., "Three-Dimensional Flow-Through Scramjet Simulation with MGD Energy-Bypass," AIAA Paper 2003-0172, Jan. 2003.

[2]Gaitonde, D., "Magnetohydrodynamic Energy-Bypass Procedure in a Three-Dimensional Scramjet," *Journal of Propulsion and Power*, Vol. 22, No. 3, 2006, pp. 498–510.

[3]Macheret, S., Ionikh, Y., Martinelli, L., Barker, P., and Miles, R., "External Control of Plasmas for High-Speed Aerodynamics," AIAA Paper 99-4853, Nov. 1999.

[4]Park, C., Bogdanoff, D., and Mehta, U., "Theoretical Performance of a Nonequilibrium MHD-Bypass Scramjet," AIAA Paper 2001-0792, Jan. 2001.

[5]Bityurin, V., Bocharov, A., and Lineberry, J., "Results of Experiments on MHD Hypersonic Flow Control," AIAA Paper 2004-2263, June 2004.

[6]Rosa, R., *Magnetohydrodynamic Energy Conversion*, McGraw–Hill, New York, 1968.

[7]Gaitonde, D., and Poggie, J., "An Implicit Technique for 3-D Turbulent MGD with the Generalized Ohms Law," AIAA Paper 2001-2736, June 2001.

[8]Gaitonde, D., "A High-Order Implicit Procedure for the 3-D Electric Field in Complex Magnetogasdynamic Simulations," *Computers and Fluids*, Vol. 33, No. 3, 2004, pp. 345–374.